MICHIGAN STATE UNIVERSITY

CYCLOTRON LABORATORY

THE NUMERICAL ACCURACY OF ^{3}He OPTICAL-MODEL CALCULATIONS AT 70 MeV

R. R. DOERING, A. I. GALONSKY, and R. A. HINRICHS

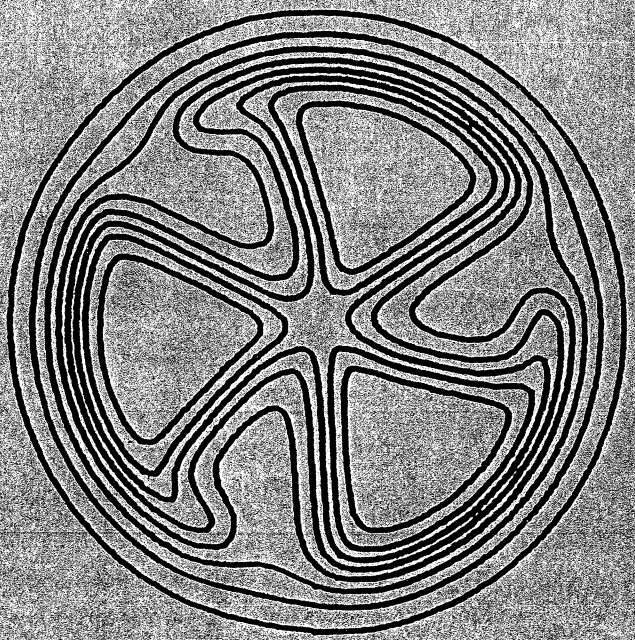

MSUCL – 61

JUNE 1972

The Numerical Accuracy of ^{3}He Optical-Model Calculations at 70 MeV*

R.R. Doering,** A.I. Galonsky, and R.A. Hinrichs

Cyclotron Laboratory, Department of Physics
Michigan State University, East Lansing, Michigan 48823

ABSTRACT

Small differential cross sections, such as those measured at back angles for 70 MeV ^{3}He elastic scattering (typically below 10^{-4} mb/sr past 130°), are difficult to calculate accurately when they result from considerable cancellation in the partial-wave sum. The codes GENOA, GIBELUMP, SNOOPY3, and DWUCK differ by as much as 2-1/2 orders of magnitude on $\sigma(\theta)$ for an optical-model potential describing ^{60}Ni(^{3}He,^{3}He)^{60}Ni scattering at 71 MeV. This calculation is repeated with a modified version of GIBELUMP for wide ranges of the parameters affecting numerical accuracy. A study of errors in scattering matrix elements and cross sections, as functions of these parameters, reveals that criteria commonly used to determine the matching radius and number of partial waves employed in optical-model calculations yield insufficient values in this case.

---

* Research supported by the National Science Foundation.
** NSF Trainee.

I. INTRODUCTION

There is increasing evidence that the well known ambiguities in optical-model potentials for complex projectiles may be at least partially resolved through analyses including large angle elastic scattering data,[1-5] especially at relatively high bombarding energies. In particular, S.M. Smith and D.A. Goldberg have noted a sensitivity of back-angle deuteron, helion, and alpha-particle elastic scattering to real well depth at incident energies above 60 MeV.[1] The characteristic feature of such data is a monotonic fall (with increasing angle) beyond the diffraction region. Such behavior is illustrated in Fig. 1, which presents 70 MeV ^{3}He elastic angular distributions taken from targets of ^{50}Ti and ^{51}V with the MSU Sector-Focused Cyclotron.[2] Similar data have been obtained by C.B. Fulmer and J.C. Hafele. They also stress the importance of the small, back-angle cross sections for suppressing ambiguities in the ^{3}He optical-model parameters.[3]

Unfortunately, we find that unusual care is required for the accurate calculation of such small cross sections, since they result from a great deal of cancellation in the partial-wave sum. The associated loss of significance can lead to difficulties of the type indicated by Fig. 2. This is a comparison of ^{60}Ni(^{3}He,^{3}He)^{60}Ni scattering at 71 MeV as calculated with the optical-model codes GENOA,[6] GIBELUMP,[7] and SNOOPY3[8] and the DWBA code DWUCK.[9] All programs used the following potential

(including the parameters with which we intended to start searches on the data of Fig. 1):

$$U(r) = U_c - V_R f(x_R) + i4W_D \frac{d}{dx_I} f(x_I), \qquad (1)$$

where $U_c = \frac{ZZ'e^2}{2R_c}\left(3-\frac{r^2}{R_c^2}\right)$ (for $r \leq R_c$),

$$U_c = \frac{ZZ'e^2}{r} \quad \text{(for } r \geq R_c\text{)},$$

$$R_c = r_c A^{1/3},$$

$$f(x) = (1+e^x)^{-1},$$

$$x_R = \frac{r-r_R A^{1/3}}{a_R},$$

and $$x_I = \frac{r-r_I A^{1/3}}{a_I},$$

with V_R=126.5 MeV, r_R=1.12 F, a_R=0.837 F, W_D=20.4 MeV, r_I=1.26 F, a_I=0.841 F, and r_c=1.3 F.[10] At forward angles, where the cross sections are large, the four codes agree quite well. However, at back angles, the cross sections are small, and there are discrepancies of as much as 2-1/2 orders of magnitude. Similar comparisons for 30 MeV helion and 50 MeV proton elastic scattering (with typical parameters) show less dramatic and negligible differences, respectively--the magnitude of the percentage disagreement being, in general, inversely related to the size of the cross section. When the ratio to Rutherford scattering is above 10^{-2}, we find little problem, but when it drops below 10^{-4}, the

calculation appears beyond the scope of many codes. This paper investigates a particular case which falls into the latter category—back-angle scattering in the aforementioned 71 MeV $^{60}Ni(^{3}He,^{3}He)^{60}Ni$ problem.

II. SOURCES OF ERROR IN OPTICAL-MODEL CALCULATIONS

Neglecting spin-dependent forces, the partial-wave expansion of the elastic scattering amplitude may be written:[11]

$$f(k,\theta) = f_c(k,\theta) + \frac{1}{2ik}\sum_{\ell=0}^{\infty}(2\ell+1)(S_\ell-1)\,e^{2i\sigma_\ell}\,P_\ell(\cos\theta) \qquad (2)$$

The most obvious source of error is the necessity to truncate the partial-wave sum after some $\ell=L_{max}$. There is also the aforementioned loss of significance due to cancellation in the sum. We may compensate for the loss of significance by calculating the individual terms more accurately. The Legendre polynomials (P_ℓ) are easily evaluated from their well known recurrence relations and expressions for $\ell=0$ and 1.[12] The Coulomb scattering amplitude (f_c) is a relatively simple function of the zero-order Coulomb phase shift (σ_0), which may be obtained along with the other σ_ℓ's by downward recursion from an asymptotic expansion for σ_L, with $\ell=L$ chosen large enough for any desired accuracy.[13] The real difficulties arise in calculating the scattering matrix elements (S_ℓ). The optical-model codes accomplish this by matching "internal" and "external" solutions of the radial Schroedinger equation at a radius $r=R_M$.

The internal solution is generated by numerically integrating the Schroedinger equation from the origin to the matching radius. The external solution is taken to be a linear combination of regular and irregular Coulomb functions. Thus, several potential sources of error are immediately evident.

If R_M is not chosen large enough to make the effects of the nuclear potential negligible, the Coulomb wave function will be a poor representation of the exact solution at that radius. Melkanoff, Raynal, and Sawada have derived[14] an approximate form of this error in the scattering matrix for the case of a Woods-Saxon potential:

$$\epsilon_F \propto \frac{Vka}{E} \exp\left[-\left(\frac{R_M - R}{a}\right)\right], \tag{3}$$

where V, R, and a are the depth, radius, and diffuseness, respectively, of the Woods-Saxon well, and E and k are the energy and wave number of the incident particle. They also give the following expressions for truncation (ϵ_T) and round-off (ϵ_R) errors in S_ℓ, which accumulate during the numerical integration:

$$\epsilon_T \propto H^4 \int_0^{R_M} \psi \frac{d^6\psi}{dr^6}\, dr \tag{4}$$

and

$$\epsilon_R \propto H^{-2} \int_0^{R_M} \psi^2\, dr, \tag{5}$$

where H is the step size and ψ is the radial wave function. Equations (4) and (5) are valid for the fourth-order Cowell[14] (also known as Fox-Goodwin[15]) method, which is widely used for

integrating second-order differential equations without a first-order term—such as the radial Schroedinger equation with a local optical-model potential. The order of the integration method refers to the finite number of terms retained in a Taylor series which represents the solution locally. The neglect of higher-order terms yields the truncation error. The round-off error results from the use of a limited number of digits in the calculation. Equations (4) and (5) indicate that both of these errors may grow with R_M. Thus, it may be possible to select too large, as well as too small, a matching radius.

The same problem is apparent for integration step size. If H is very small, the truncation error will be small, but the round-off error, large, and vice-versa. Hopefully, some domain of H (and R_M) will always exist for which these errors in the scattering matrix elements remain suitably bounded.

The scattering matrix also receives errors from the Coulomb wave functions, which may be evaluated by a variety of techniques, each fraught with unique difficulties. For relatively small values of the Coulomb parameter $\eta(=\mu ZZ'e^2/k\hbar^2)$ and large values of $\rho(=kr)$, the Coulomb functions are commonly calculated with recursion relations and asymptotic expansions.[16] Except for a normalization factor, the regular Coulomb functions (F_ℓ) may be obtained by downward recursion from $F_{\lambda'+1}=0$ and $F_{\lambda'}=\delta$, an arbitrary "small" number. As in the case of Coulomb phase shifts, a particular $\ell=\lambda'$ is chosen which determines the accuracy at lower ℓ's. The normalization may

be found by requiring the Wronskian of the zero-order Coulomb functions to equal 1. One of the required derivatives, F_0', is simply related to F_0 and F_1. Unfortunately, the asymptotic series for the zero-order irregular function and its derivative are only semi-convergent. If summing until the series begin to diverge does not give the desired accuracy, they may be summed at a larger radius (ρ), where the initial convergence is more rapid. The resulting values may then be used to start a numerical integration of the Schroedinger equation, containing only the Coulomb potential, inward to the matching radius. At this point upward recursion will generate the irregular Coulomb functions (G_ℓ) for the higher ℓ's. Upward recursion preserves significance for the irregular functions, since they generally grow in magnitude with increasing ℓ, opposite to the behavior of the regular functions.

We have mentioned the major sources of error in a typical optical-model calculation of an elastic scattering amplitude. The errors in the partial-wave amplitudes each have associated "numerical accuracy parameters" (e.g., R_M), which control particular approximations. We seek values of these parameters which yield very accurate individual amplitudes, a few significant figures of which will survive the extreme cancellation in the partial-wave sum for small cross sections.

III. ERRORS IN THE SCATTERING MATRIX

The code GIBELUMP has been modified so that the afore-mentioned numerical accuracy parameters may be specified

externally and varied over wide ranges. If we simplify matters by always evaluating the asymptotic expansions of the Coulomb functions at the matching radius (i.e., setting $\mathcal{R}=R_M$), we are left with four such parameters: L, $\mathcal{S}$, R_M, and H. The first pair is rather easy to set, since the associated errors diminish as L and $\mathcal{S}$ become larger. Therefore, we merely need to increase these parameters until the scattering amplitudes remain constant to the number of significant figures desired. However, the matching radius and integration step size cannot be dealt with in such an elementary manner. As we have seen, there are errors coupled to R_M and H which have opposite dependences on these parameters. Thus, the net error in each partial-wave amplitude may be a complicated function of the matching radius and integration step size. To facilitate selection of R_M and H for our ^{3}He elastic scattering calculation, we have investigated this function (for several values of ℓ) at matching radii between 10 F and 30 F and step sizes from 0.0075 F to 0.2 F. Since these two parameters enter a partial-wave amplitude only through S_ℓ, it is sufficient to consider errors in the scattering matrix alone. Also, since the Coulomb parameter is small ($\eta<2$) for our case, we do not expect these errors to be significantly affected by the calculation of Ricatti-Bessel[17] rather than Coulomb functions (i.e., setting $\eta=0$). Thus, we have omitted the Coulomb potential from the computations discussed in this section. This enables us to also calculate S_ℓ's from second-order Born approximation solutions to the coupled integral equations for the phase shifts.[18]

Such calculations were performed with the code PWBA2.[19] The scattering matrix elements in Table I were obtained with PWBA2 and the modified GIBELUMP (with H=0.0125 F, R_M=25.0 F, ℓ=100, and L=101). Both codes employed the previously listed ^3He-^{60}Ni potential (except for the Coulomb term) at an incident ^3He energy of 71 MeV. Since PWBA2 and GIBELUMP use entirely different methods of arriving at the S_ℓ's, the extent to which they agree indicates a lower bound on the accuracy of each. As the partial-wave number increases, the Born series converges more rapidly (for suitable potentials), and it appears that PWBA2 is accurate to ≥8 decimal places for $\ell \geq 40$. Thus, we may define errors in the scattering matrix elements calculated with the modified GIBELUMP (which will be meaningful if larger than about 10^{-8} for $\ell \geq 40$) by:

$$\text{Re } \varepsilon_\ell = |\text{Re } S_\ell^{\text{PWBA2}} - \text{Re } S_\ell^{\text{GIBELUMP}}|$$

and

$$\text{Im } \varepsilon_\ell = |\text{Im } S_\ell^{\text{PWBA2}} - \text{Im } S_\ell^{\text{GIBELUMP}}|.$$

Figure 3 shows the dependence of these errors on matching radius for H=0.015 F and ℓ=40, 50, and 60. The scattering matrix elements are extremely close to unity, and the corresponding errors almost constant, until R_M reaches the classical impact parameter $R_\ell = \ell/k$ ($k \simeq 3$ F^{-1}) for each partial wave. Farther out we observe an exponential decrease, as predicted by Eq. (3) for the finite matching radius error. The region of minimum observable error extends from about 22 F to 25 F, beyond which an exponentially

increasing error becomes measurable. This confirms our previous speculation that R_M can be chosen too large.

There appear to be two major sources of error contributing to the ε_ℓ's. One dominates at small matching radii and decreases exponentially with R_M, eventually being overtaken (somewhere outside 20 F) by the other, which increases exponentially. Since GIBELUMP employs a fourth-order Cowell numerical integration algorithm, Eqs. (4) and (5) may be used to interpret the dependence of the scattering matrix errors on integration step size (for fixed matching radii). With R_M=15 F, Fig. 4 indicates that the ε_ℓ's are independent of step size. Thus, the major source of error for $R_M \lesssim 20$ F does not behave like truncation [Eq. (4)] or round-off [Eq. (5)]. However, its behavior as a function of H (as well as R_M) is consistent with Eq. (3), which describes the error due to finite matching radius. For R_M=25 F, Fig. 5 reveals scattering matrix errors growing as the fourth power of integration step size. This implies that the dominant source of error at large matching radii is accumulating truncation in the numerical integration. If, instead, the main source were round-off, the characteristic H^{-2} dependence would be observed. Compilation of the modified GIBELUMP in double precision on a computer (the MSU Cyclotron Laboratory XDS Sigma-7) with 32-bit words is largely responsible for the lack of noticeable round-off error.

Similar studies have been made for ℓ=0 and 10 by using S_ℓ's from the modified GIBELUMP (with R_M=25.0 F and H=0.0125 F) instead of PWBA2. The redefined "errors" in the scattering matrix show the same behavior as functions of R_M and H for low partial-wave number as ε_{40}, ε_{50}, and ε_{60} in Figs. 3-5.

IV. ERRORS IN THE DIFFERENTIAL CROSS SECTION

Thus far we have determined that a matching radius of about 25 F and the smallest integration step size consistent with our 2000 step maximum (computer memory limited), i.e., H≃0.0125 F, minimize the errors in our partial-wave amplitudes. The total error in the full elastic scattering amplitude also contains contributions from the aforementioned loss of significance (due to cancellation in the partial-wave sum) and neglect of terms [in Eq. (2)] for ℓ greater than some L_{max}. Table I indicates that, much beyond ℓ=60, the scattering matrix elements will differ from unity by less than their probable errors. Thus, there are vanishing returns from selecting L_{max} above 60. Also, it is found that Coulomb functions calculated with the modified GIBELUMP for ℓ=60, η=1.81733, and ρ=75 (r≃25) remain constant to 12 significant figures when values greater than the previously used $\mathcal{L}$=100 and L=101 are tried. Note that this does not imply an accuracy of anything like one part in a trillion for the F_ℓ's and G_ℓ's, since the radius at which the semi-convergent asymptotic series are summed ($\mathcal{R}$) is also important. A comparison of Coulomb functions from the

modified GIBELUMP (for η=0) with Ricatti-Bessel functions from RBESS2[20] suggests an accuracy more on the order of one part in a million. However, this will clearly not be improved by selecting values of $\mathscr{A}$ and L larger than 100 and 101, respectively. Thus, we will refer to the following set as our "optimum numerical accuracy parameters": R_M=$\mathscr{R}$=25.0 F, H=0.0125 F, L_{max}=60, $\mathscr{A}$=100, and L=101. Assuming they yield a sufficiently accurate scattering amplitude at 71 MeV, for the full (including Coulomb) ^{3}He-^{60}Ni potential, allows us to define an "error" in the differential cross section by:

$$\varepsilon(\theta) = \frac{|\sigma_0(\theta)-\sigma_T(\theta)|}{\sigma_0(\theta)} \times 100\%,$$

where $\sigma_0(\theta)$ is calculated by the modified GIBELUMP with the optimum parameters and $\sigma_T(\theta)$, with some test set. A few values of $\sigma_0(\theta)$ are listed in Table II.

Investigating this error as a function of R_M, H, and L_{max}, for several scattering angles (θ) of interest, affords a means of minimizing calculation time by selecting parameters which yield sufficient, but not greater, accuracy than required. For example, it might be a very inefficient use of computer time to calculate cross sections accurate to 6 significant figures while searching on data with 10% experimental errors. In studying $\varepsilon(\theta)$, the test parameters were varied one at a time, the others remaining fixed at their optimum values.[21]

All optical-model codes have limits on the values of the numerical accuracy parameters. Most also have internal criteria which choose some of them automatically. The codes of Fig. 2 selected matching radii between 10 F and 13 F for 71 MeV ^{3}He scattering from the potential defined by Eq. (1). The original GIBELUMP sets R_M equal to the radius plus 7 times the diffuseness of whichever term in the potential gives the largest value. GENOA does the same except for using 9 times the diffuseness. If it is not externally specified, SNOOPY3 defines the matching radius to be the point at which the ratio of nuclear to Coulomb potential is less than 0.005/k. DWUCK adds the largest radius (of any term in the potential) to 9.2 times the largest diffuseness. Figure 6 illustrates that these criteria yield matching radii which are too small for the modified GIBELUMP to accurately calculate our back-angle cross sections. Also note that the errors are growing exponentially beyond 27 F.

Hodgson has suggested that each unit of ρ be divided into 10 integration steps.[22] This gives a step size of about 0.03 F for the 71 MeV helions. Figure 7 indicates that this choice corresponds to only 0.1% errors in $\sigma(\theta)$, even at the largest angles. However, of the 4 codes we have examined, only SNOOPY3 has the capability of selecting H (with a more complicated method than Hodgson's). For the calculation shown in Fig. 2, SNOOPY3 picked H=0.05 F, the smallest value which it allows. The other 3 codes were given the commonly used 0.1 F integration step size, which, alone, would be responsible for up to 10% errors in the cross section (Fig. 7).

Criteria similar to Hodgson's for the number of partial waves[22] have been widely incorporated into optical-model codes. GENOA, the original GIBELUMP, and SNOOPY3 all truncate the partial-wave sum after some condition closely related to $|1-S_\ell|<10^{-N}$ is satisfied. For GENOA and the original GIBELUMP N=4, and for SNOOPY3 N=3, if not otherwise specified. Each of these codes used $33\leq L_{max}\leq 37$ for the calculations of Fig. 2. The DWBA code DWUCK requires the user to input the number of partial waves to be included in the sum. For this comparison with the optical-model codes, we set $L_{max}=35$ for DWUCK. However, from Fig. 8 we conclude that enormous errors in the small, back-angle cross sections can result from the neglect of partial waves above the thirty-fifth.

V. CONCLUSION

The disagreement between codes depicted in Fig. 2 may be greatly diminished by the use of improved values for the numerical accuracy parameters. In particular, increasing (within limits) the matching radii and numbers of partial waves from the values employed in the original GIBELUMP, GENOA, SNOOPY3, and DWUCK calculations of Fig. 2 would yield cross sections approaching the angular distribution obtained from the modified GIBELUMP with the optimum numerical accuracy parameters. To a lesser extent, decreasing the integration step sizes would also help.

Figure 9 illustrates, as an example, the effect of using DWUCK with R_M=20.0 F, L_{max}=60, and H=0.05 F, rather than R_M=12.65 F, L_{max}=35, and H=0.10 F as in Fig. 2. In both of these figures the solid lines are $\sigma_0(\theta)$ as calculated with the modified GIBELUMP and the optimum numerical accuracy parameters (e.g., R_M=25.0 F, L_{max}=60, and H=0.0125 F). The vastly closer agreement of the GIBELUMP and DWUCK calculations in Fig. 9 than in Fig. 2 provides further evidence that parameters approaching our optimum values yield considerably greater numerical accuracy than those commonly used in optical-model codes for ^{3}He elastic scattering, especially for the small, back-angle cross sections which occur for bombarding energies on the order of 70 MeV. Note that the pronounced, back-angle oscillations in the original GIBELUMP, GENOA, SNOOPY3, and DWUCK angular distributions of Fig. 2 are replaced (except for the "glory peak"[23]) by a smooth fall in the more accurate calculations. This behavior bears a strong qualitative resemblance to the data in Fig. 1 and may be expected to facilitate the optical-model analyses.

This investigation has concentrated on a particular example of elastic scattering. No attempt has been made to suggest new criteria for the numerical accuracy parameters which would be adequate over wide ranges of projectiles, targets, and energies. Each case deserves individual attention. However, we trust that these results are indicative of the numerical difficulties associated with using standard optical-model codes to calculate small cross sections.

ACKNOWLEDGEMENTS

We would like to thank C.B. Fulmer for supplying us with test GENOA calculations and optical-model analyses of his data prior to publication. We are also grateful to W.F. Steele for the use of integration and Bessel function subroutines and to R. Bortins for general assistance.

REFERENCES

1. S.M. Smith and D.A. Goldberg, Bull. Am. Phys. Soc. 17, 591(1972).
2. R.A. Hinrichs, R.R. Doering, and A. Galonsky, Bull. Am. Phys. Soc. 16, 628(1971); to be published.
3. C.B. Fulmer, Oak Ridge National Laboratory, and J.C. Hafele, Washington University, to be published.
4. P.P. Urone, L.W. Put, B.W. Ridley, and G.D. Jones, Nucl. Phys. A167, 383(1971).
5. J.W. Luetzelschwab and J.C. Hafele, Phys. Rev. 180, 1023 (1969).
6. Optical-model search code written by F.G. Perey, Oak Ridge National Laboratory.
7. Optical-model search code written by F.G. Perey, ORNL, and modified by R.M. Haybron, Cleveland State University.
8. Optical-model search code written by P. Schwandt, Indiana University.
9. Distorted wave Born approximation code written by P.D. Kunz, University of Colorado.
10. Optical-model parameters obtained from C.B. Fulmer, ORNL, in a private communication.
11. M.A. Preston, Physics of the Nucleus (Addison-Wesley Publishing Co., Inc., Reading, Mass., 1962), p. 630.
12. J.D. Jackson, Classical Electrodynamics (John Wiley and Sons, Inc., New York, 1962), Chap. 3.

13. P.E. Hodgson, The Optical Model of Elastic Scattering (Oxford University Press, London, 1963), Chap. 2, p. 35.

14. M.A. Melkanoff, T. Sawada, and J. Raynal, Meth. Comp. Phys. 6, 1(1966).

15. L. Fox and E.T. Goodwin, Proc. Cambridge Phil. Soc. 45, 373(1949).

16. I.A. Stegun and M. Abramowitz, Phys. Rev. 98, 1851(1955); C. Fröberg, Revs. Mod. Phys. 27, 399(1955).

17. M. Abramowitz and I.A. Stegun, Handbook of Mathematical Functions (National Bureau of Standards, Washington, D.C., 1965), Chap. 10, p. 445.

18. P. Roman, Advanced Quantum Theory (Addison-Wesley Publishing Co., Inc., Reading, Mass., 1965), Chap. 3, p. 166.

19. Second-order Born approximation code written by R.R. Doering.

20. Ricatti-Bessel function code based on algorithm 236— W. Gautschi, Commun. ACM 7, 479(1964); translated into FORTRAN by W.F. Steele, Michigan State University, and extended to the irregular functions by R.R. Doering.

21. For matching radii greater than 25 F, H=0.015 F was used rather than H=0.0125 F.

22. P.E. Hodgson, op. cit., p. 43.

23. R.G. Newton, Scattering Theory of Waves and Particles (McGraw-Hill Book Co., Inc., New York, 1966).

FIGURE CAPTIONS

1. 70 MeV ^{3}He elastic scattering data taken from targets of ^{50}Ti, and ^{51}V.
2. Comparison of elastic scattering calculated with 4 codes from the same potential. The reference lines are from a more accurate calculation with a modified version of GIBELUMP which employed the optimum numerical accuracy parameters defined in the text.
3. Dependence of errors in scattering matrix elements on matching radius for a 0.015 integration step size.
4. Dependence of errors in scattering matrix elements on integration step size for a 15 F matching radius.
5. Dependence of errors in scattering matrix elements on integration step size for a 25 F matching radius.
6. Dependence of errors in $\sigma(\theta)$ on matching radius, with other accuracy parameters at optimum values—e.g., H=0.0125 F and L_{max}=60.
7. Dependence of errors in $\sigma(\theta)$ on integration step size, with other accuracy parameters at optimum values—e.g., R_M=25.0 F and L_{max}=60.
8. Dependence of errors in $\sigma(\theta)$ on the number of partial waves included in the sum, with other accuracy parameters at optimum values—e.g., R_M=25.0 F and H=0.0125 F.
9. Elastic scattering calculated with the modified GIBELUMP, for the optimum numerical accuracy parameters defined in the text, and with DWUCK, for parameters as near these as possible. Compare with Fig. 2.

Table I. Comparison of scattering matrix elements calculated with the modified GIBELUMP (optical-model code) and PWBA2 (second-order Born approximation code). The errors in Figs. 4-6 are relative to these PWBA2 results for partial-wave numbers of 40, 50, and 60.

	Real S_ℓ		Imaginary S_ℓ	
ℓ	GIBELUMP	PWBA2	GIBELUMP	PWBA2
20	.12941772	.00101740	.09446676	.28783675
21	.25494459	.20751226	.15728529	.27749207
22	.40959841	.39774516	.18916798	.25166682
23	.55919313	.55834389	.18627662	.21455524
24	.68339913	.68449549	.16157908	.17316819
25	.77761587	.77846355	.12928026	.13372584
30	.96526366	.96527341	.02580755	.02583216
35	.99466337	.99466340	.00409806	.00409809
40	.99918378	.99918378	.00062544	.00062538
45	.99987590	.99987590	.00009436	.00009432
50	.99998123	.99998123	.00001416	.00001414
55	.99999717	.99999717	.00000212	.00000211
60	.99999958	.99999958	.00000032	.00000031

Table II. 71 MeV ^{3}He elastic scattering from ^{60}Ni as calculated with the modified GIBELUMP for the optical-model and optimum numerical accuracy parameters defined in the text. The errors in Figs. 6-8 have been determined with respect to these cross sections at 90.0, 150.0, 170.0, and 180.0 degrees.

$\theta_{c.m.}$ (deg)	$\sigma_{c.m.}$ (mb/sr)
10.0	4.942×10^{3}
20.0	9.444×10^{1}
30.0	1.334×10^{1}
40.0	7.929×10^{-1}
50.0	1.342×10^{-1}
60.0	1.849×10^{-1}
70.0	7.996×10^{-2}
80.0	2.551×10^{-2}
90.0	8.972×10^{-3}
100.0	2.970×10^{-3}
110.0	7.659×10^{-4}
120.0	2.217×10^{-4}
130.0	8.363×10^{-5}
140.0	2.818×10^{-5}
150.0	1.112×10^{-5}
160.0	4.462×10^{-6}
170.0	2.241×10^{-6}
180.0	2.596×10^{-5}

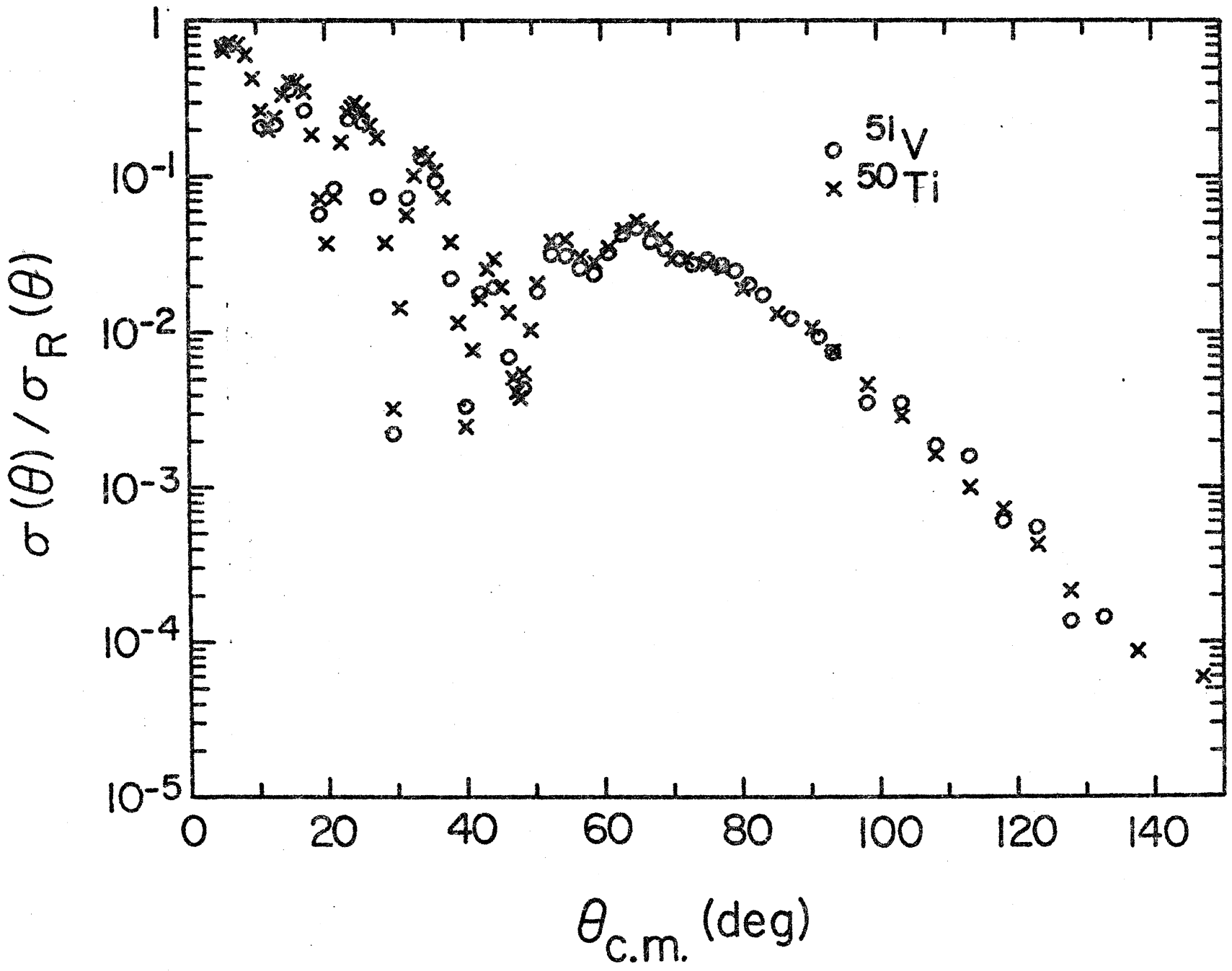
1
10^{-1}
10^{-2}
10^{-3}
10^{-4}
10^{-5}
$\sigma(\theta)/\sigma_R(\theta)$
0
20
40
60
80
100
120
140
$\theta_{c.m.}$ (deg)
^{51}V
^{50}Ti

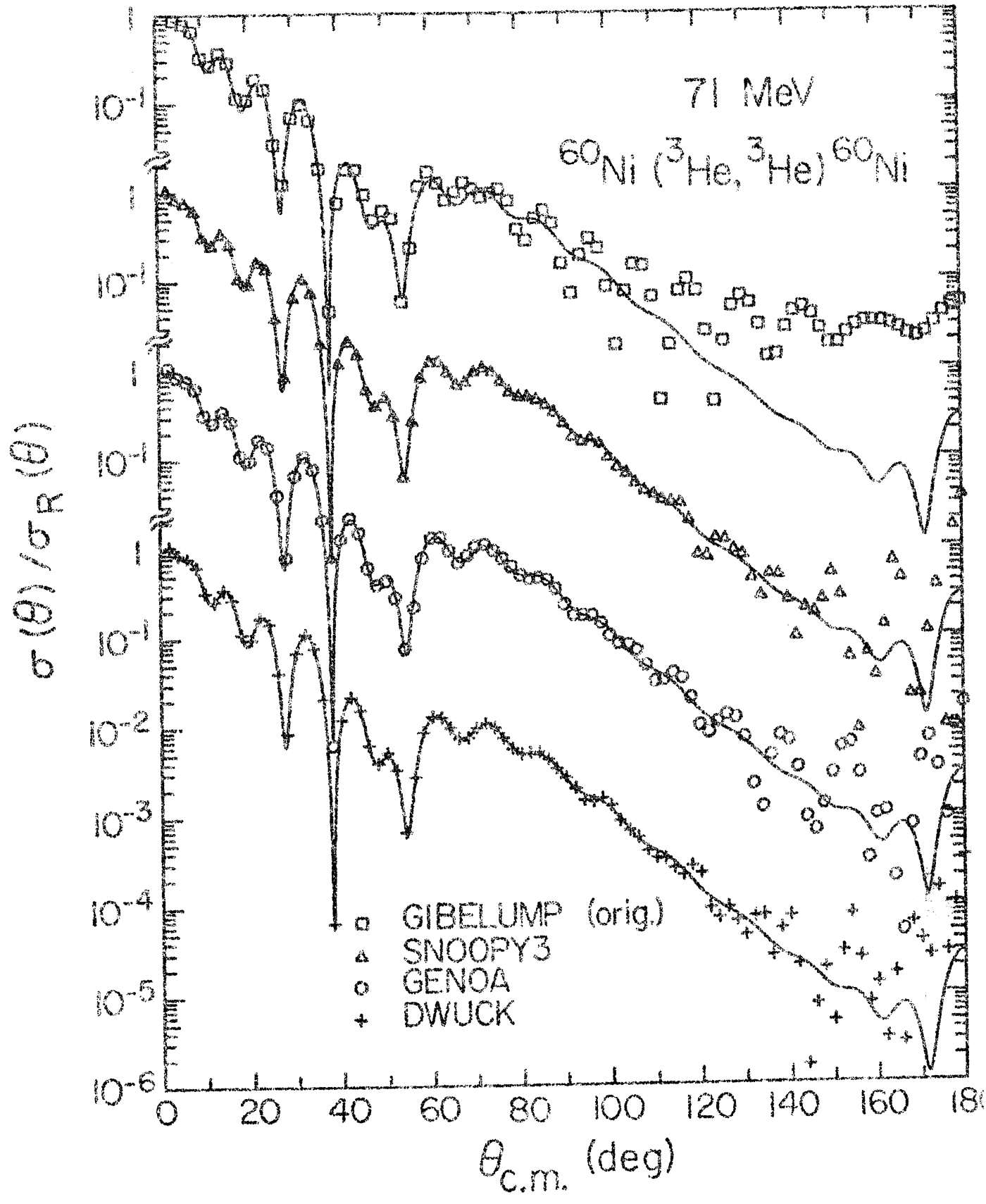
71 MeV
^{60}Ni (^{3}He, ^{3}He) ^{60}Ni
GIBELUMP (orig.)
SNOOPY3
GENOA
DWUCK
$\sigma(\theta)/\sigma_R(\theta)$
$\theta_{c.m.}$ (deg)
1
10^{-1}
10^{-2}
10^{-3}
10^{-4}
10^{-5}
10^{-6}
0
20
40
60
80
100
120
140
160

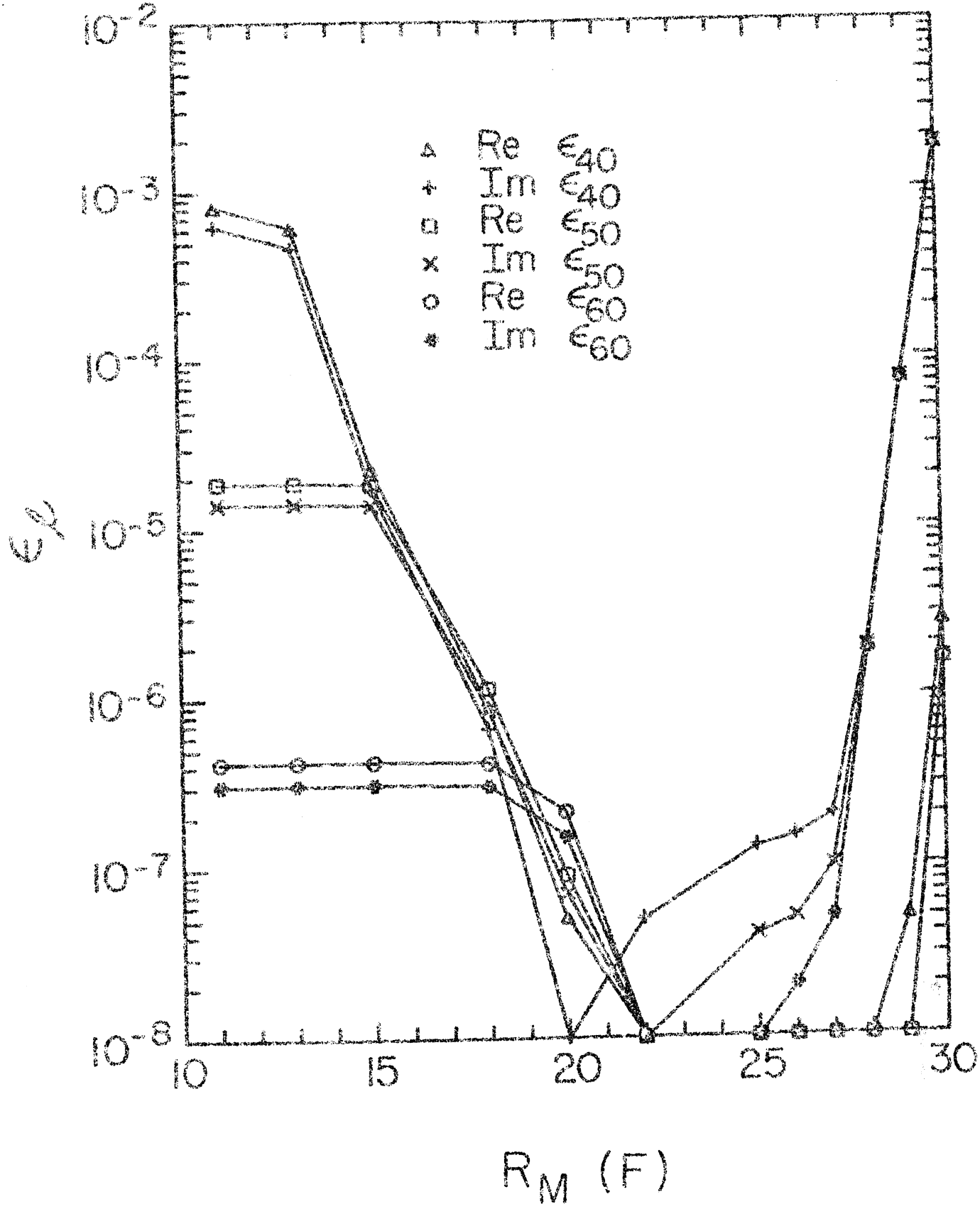
Re ϵ_{40}
Im ϵ_{40}
Re ϵ_{50}
Im ϵ_{50}
Re ϵ_{60}
Im ϵ_{60}
ϵ^2
10^{-2}
10^{-3}
10^{-4}
10^{-5}
10^{-6}
10^{-7}
10^{-8}
10
15
20
25
30
R_M (F)

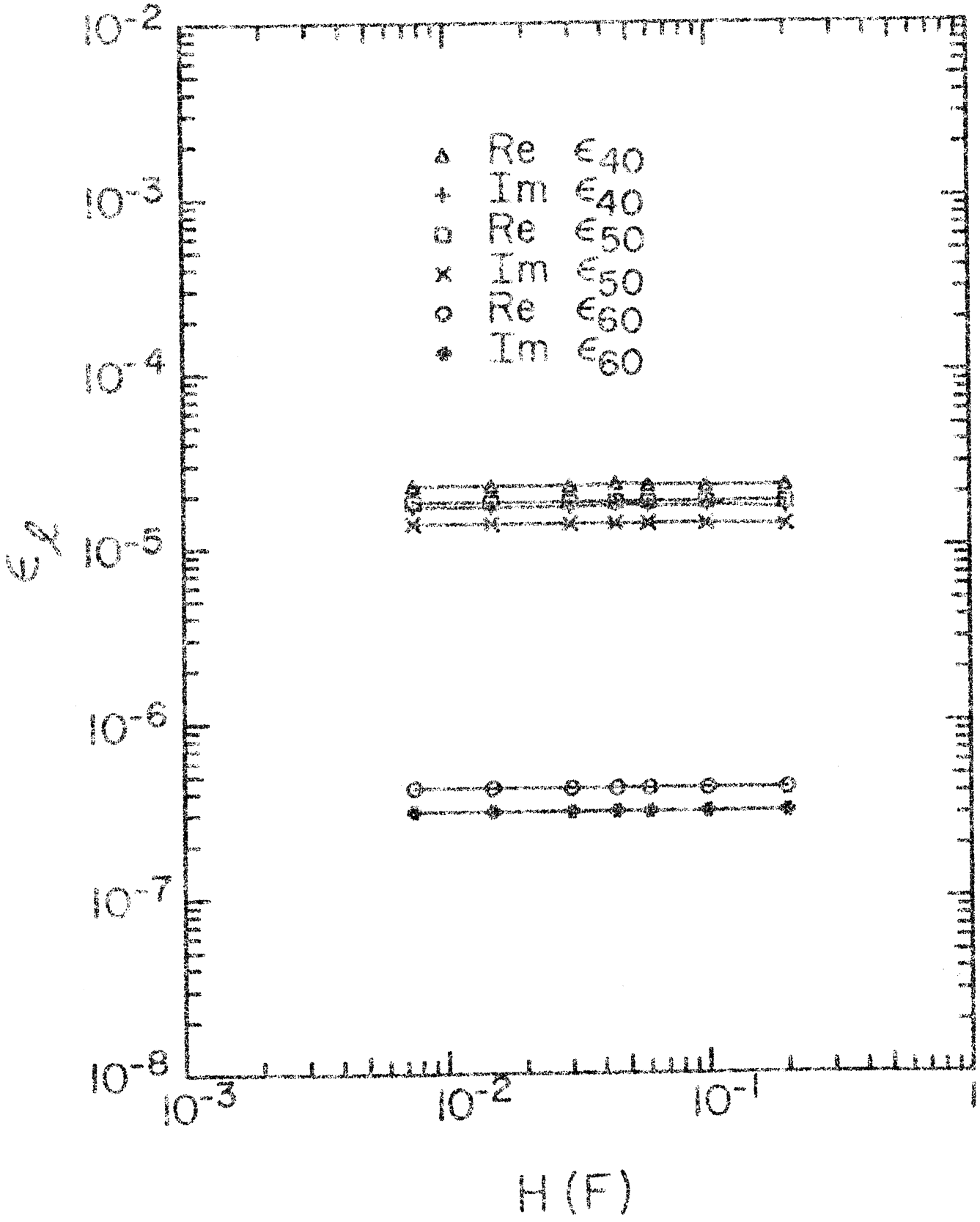
Re ϵ_{40}
Im ϵ_{40}
Re ϵ_{50}
Im ϵ_{50}
Re ϵ_{60}
Im ϵ_{60}
10^{-2}
10^{-3}
10^{-4}
10^{-5}
10^{-6}
10^{-7}
10^{-8}
ϵ_{ij}
10^{-3}
10^{-2}
10^{-1}
H (F)

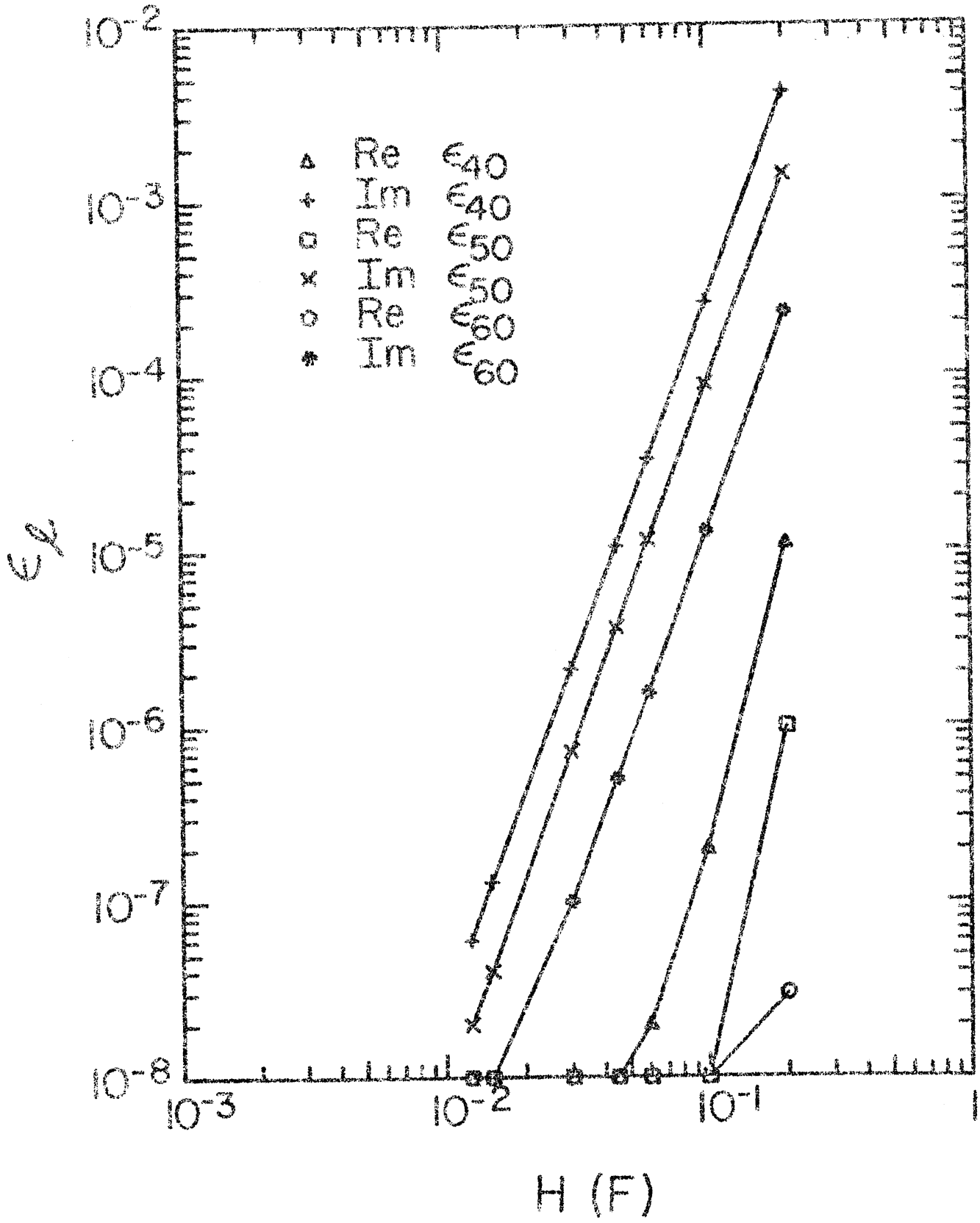
10^{-2}
10^{-3}
10^{-4}
10^{-5}
10^{-6}
10^{-7}
10^{-8}
ϵ_2
Re ϵ_{40}
Im ϵ_{40}
Re ϵ_{50}
Im ϵ_{50}
Re ϵ_{60}
Im ϵ_{60}
10^{-3}
10^{-2}
10^{-1}
1
H (F)

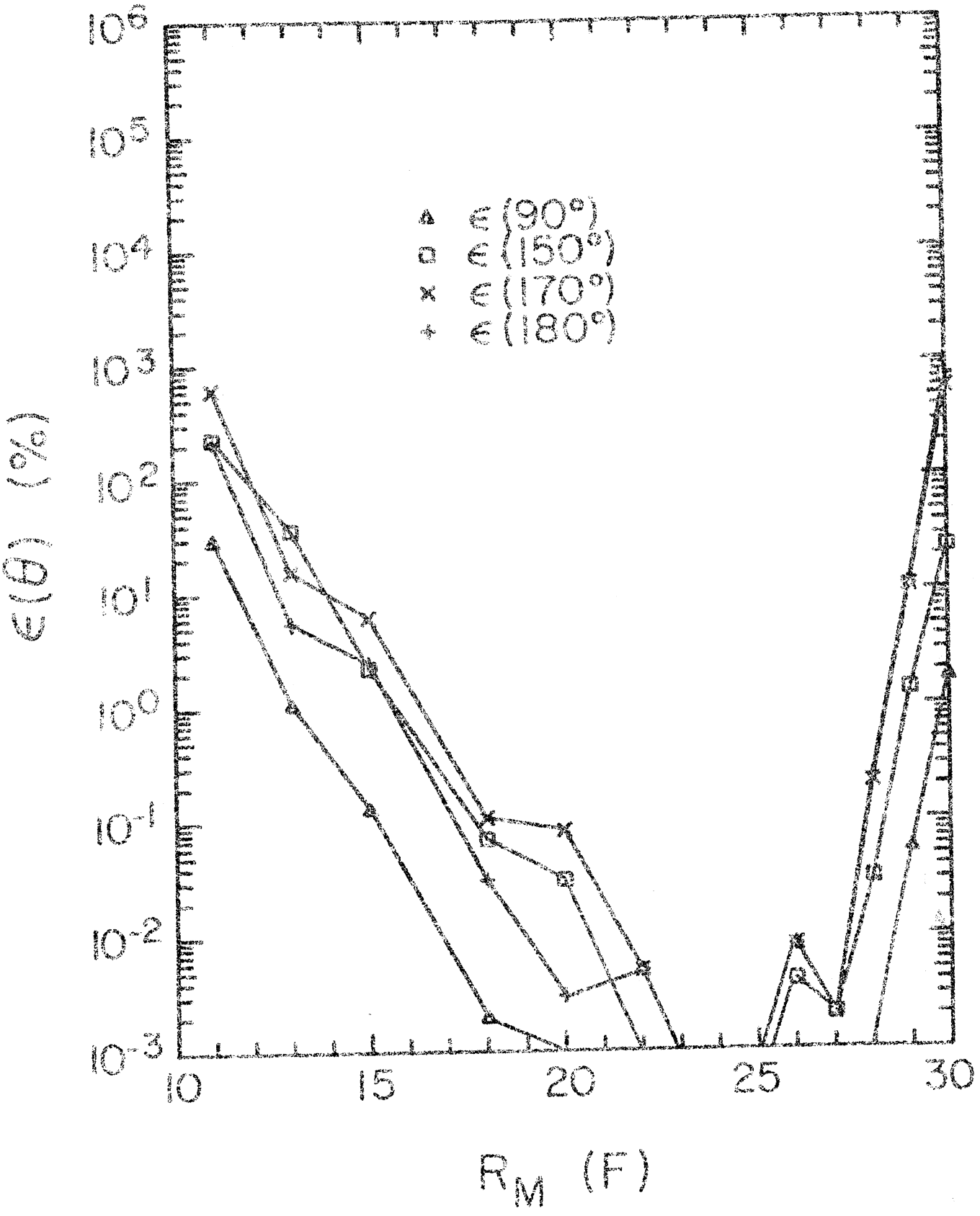
10^6
10^5
10^4
10^3
10^2
10^1
10^0
10^{-1}
10^{-2}
10^{-3}
$\epsilon(\beta)$ (%)
ϵ (90°)
ϵ (150°)
ϵ (170°)
ϵ (180°)
10
15
20
25
30
R_M (F)

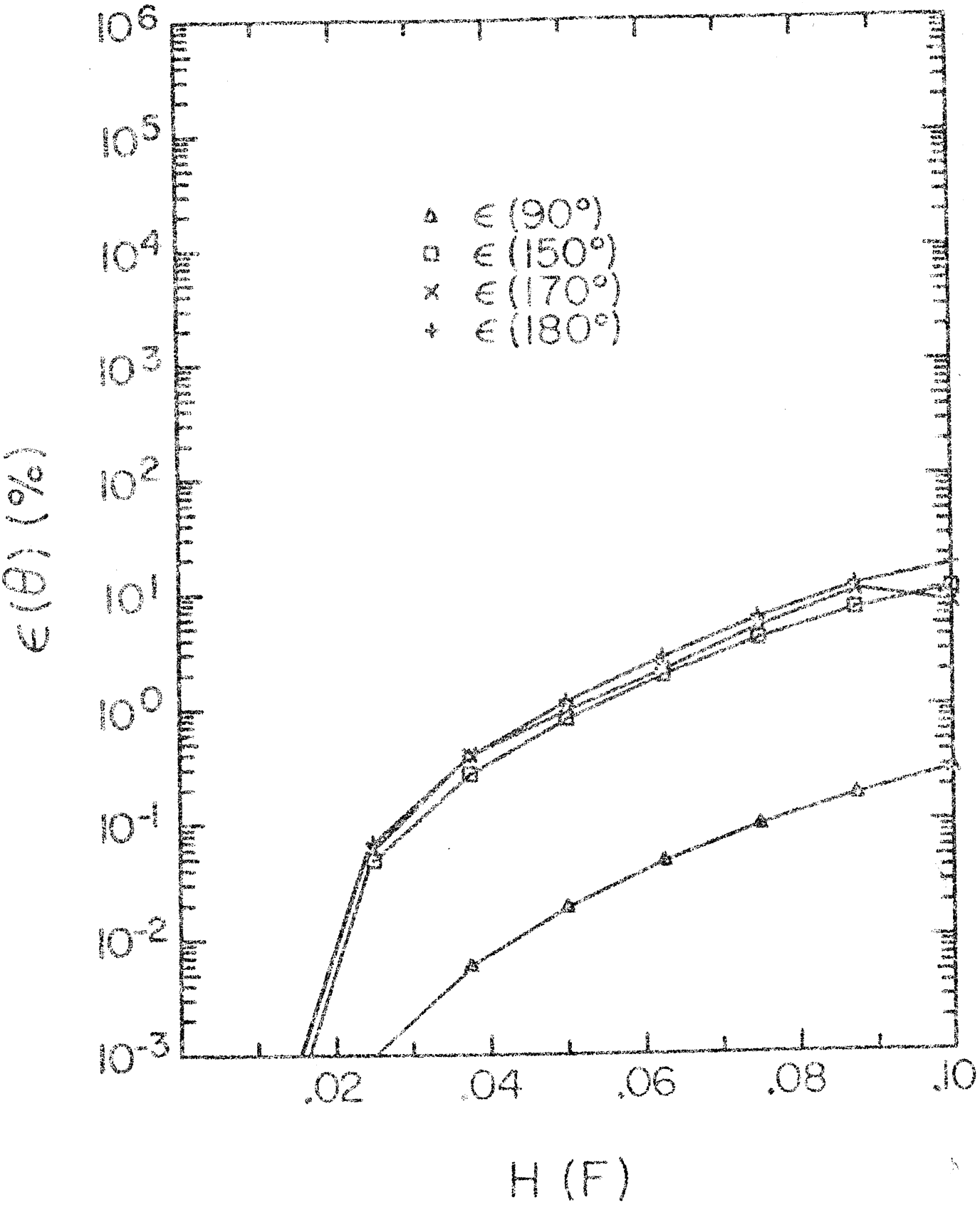
ε (θ) (%)
10^6
10^5
10^4
10^3
10^2
10^1
10^0
10^-1
10^-2
10^-3
.02
.04
.06
.08
.10
H (F)
ε (90°)
ε (150°)
ε (170°)
ε (180°)

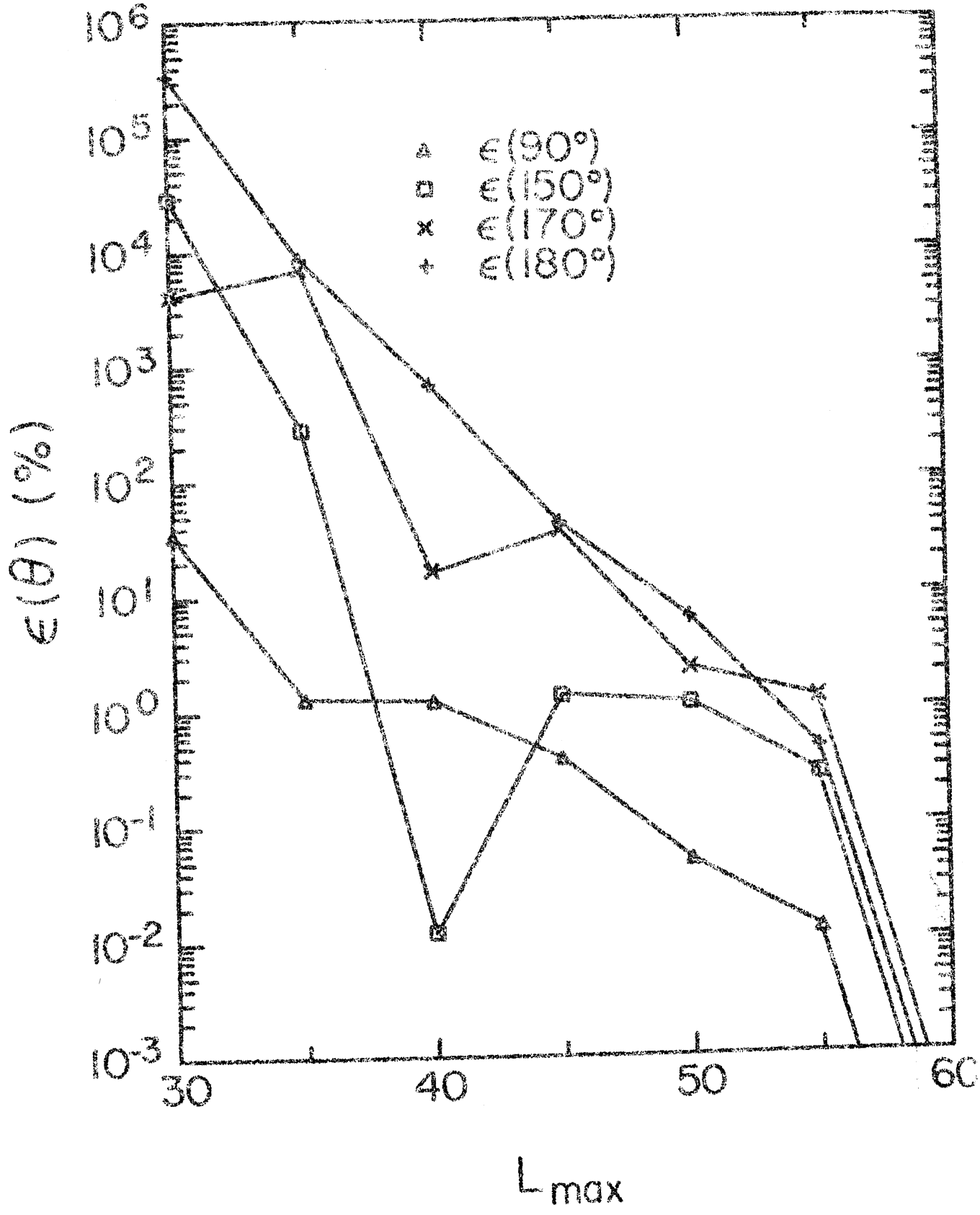
ε(90°)
ε(150°)
ε(170°)
ε(180°)
ε(θ) (%)
10^6
10^5
10^4
10^3
10^2
10^1
10^0
10^-1
10^-2
10^-3
30
40
50
60
L max

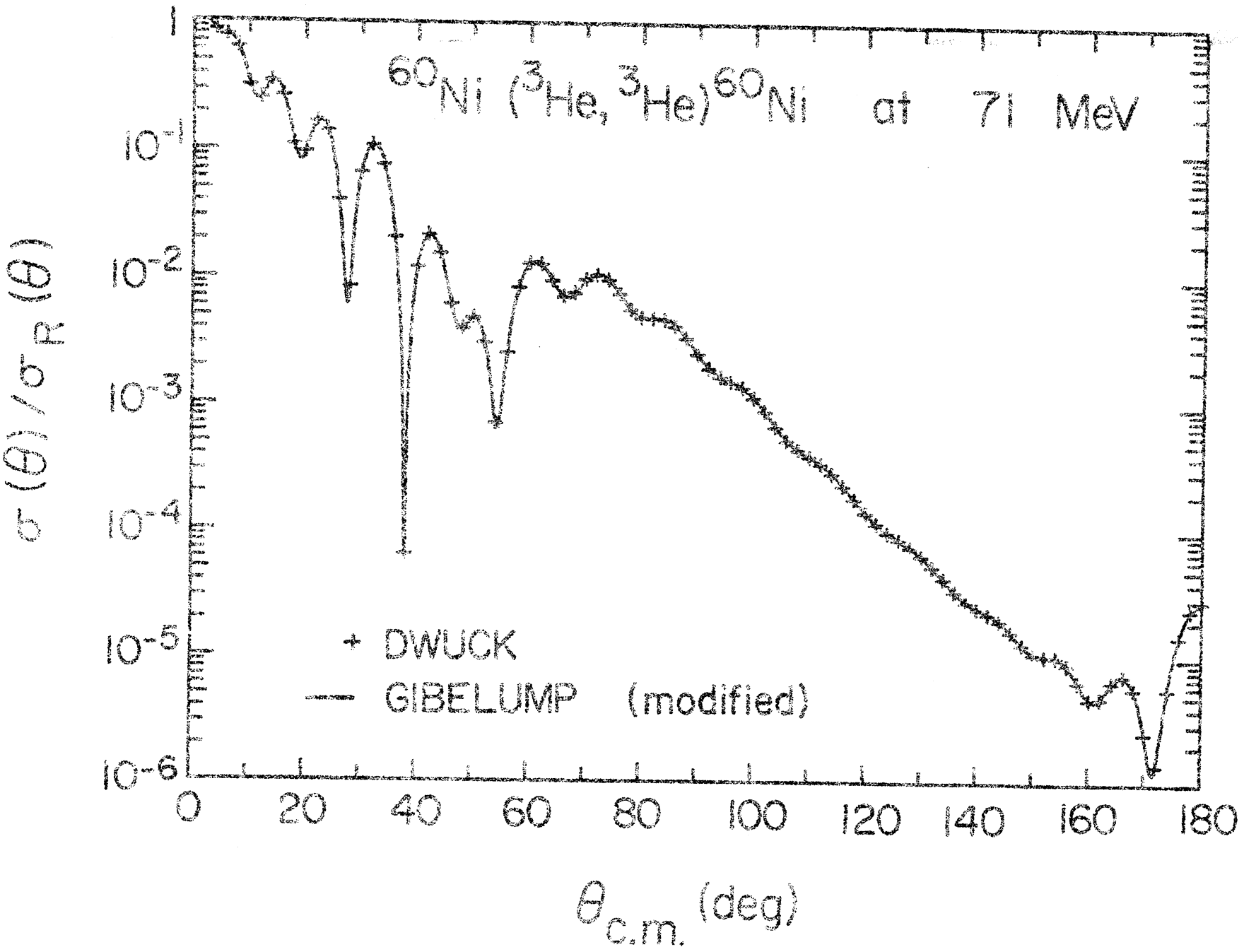
^{60}Ni (^{3}He, ^{3}He)^{60}Ni at 71 MeV
+ DWUCK
— GIBELUMP (modified)
$\sigma(\theta)/\sigma_R(\theta)$
$\theta_{c.m.}$ (deg)
1
10^{-1}
10^{-2}
10^{-3}
10^{-4}
10^{-5}
10^{-6}
0
20
40
60
80
100
120
140
160
180